Post-magmatic alteration in eudialyte from the North Qôroq centre, South Greenland

IAN M. COULSON

School of Earth Sciences, The University of Birmingham, Edgbaston, Birmingham B15 2TT, England

Abstract

The North Qôroq centre comprises a series of nested nepheline syenite intrusions and forms part of the mid-late Proterozoic Gardar province of South Greenland. Within the centre fractionation has produced varied rock types ranging from augite-syenite to lujavrite, a eudialyte microsyenite. Samples of eudialyte from the lujavrites of unit SN1B of the centre show evidence for two-stage alteration. This alteration ranges from slight modification along crystal margins to complete breakdown and replacement by new pseudomorphing phases. Modification to crystal margins is accompanied by increasing Nb and Zr contents and is related to metasomatism produced by the intrusion of younger syenite units of the North Qôroq centre. More extensive alteration is as a result of metasomatism followed by lower-temperature supergene alteration. Simplified reactions for this breakdown include eudialyte + metasomatic fluid = allanite + nepheline; eudialyte + metasomatic fluid = titanite + aegirine + møsandrite + wöhlerite; eudialyte + fluid = zirfesite + fluid. Mass balance calculations for altered compared with unaltered samples of lujavrite show that alteration took place at approximately constant volume with an overall increase in Fe (+2.41 g/100g), Si and K (+0.65 and +0.61 g/100g), whilst Na (−2.67 g/100g) and all trace elements, particularly La, Y, Nb and Zr (−5.6 to −166 g/10000g) are lost from the system.

KEYWORDS: eudialyte, zirfesite, alteration, metasomatism, lujavrite, Igaliko, Gardar, Greenland.

Introduction

The North Qôroq centre comprises a series of nested nepheline syenite intrusions and forms part of the Igaliko complex in the mid–late Proterozoic Gardar province of South Greenland (Upton and Emeleus, 1987). The field relationships and petrography of the centre are described by Emeleus and Harry (1970). Within unit SN1B of the centre, several large irregular shaped bodies of lujavrite have been found and are described by Coulson and Chambers (1996). This rock type, a eudialyte microsyenite, is only found in three of the Gardar intrusions and is thought to have formed as a result of accumulation of residual nepheline syenitic magma underneath large country-rock xenoliths (cf. Jones and Larsen, 1985).

Exotic light rare-earth element (*LREE*)-minerals and *LREE*-bearing phases, such as eudialyte, are a major feature of alkaline and agpaitic provinces (e.g. Lovozero, Kola Peninsula), and occur with many unusual minerals such as møsandrite, wöhlerite and nacareniobsite (Vlasov *et al.*, 1966; Mellini and Merlino, 1979; Petersen *et al.*, 1989; Khomyakov, 1990; Jones *et al.*, 1996). This paper presents new evidence for two-stage alteration of eudialyte from the North Qôroq centre.

Description

The samples of eudialyte studied are from one of the largest units within the North Qôroq centre. This unit shows extreme effects of fractional crystallization with a marginal augite syenite and a peralkaline (agpaitic) core of lujavrite. The unit has undergone partial auto-metasomatism and metasomatism by later syenite units of the North Qôroq centre and the other Igaliko intrusions (Coulson and Chambers, 1996).

Eudialyte

Eudialyte ($Na_3(Ca,REE)_2(Fe,Mn)Zr(Si_3O_9)_2(OH,Cl,F)$) was identified in several rock types in North Qôroq including sodalite syenite, lujavrite,

Mineralogical Magazine, Vol. 61, February 1997, pp. 99–109

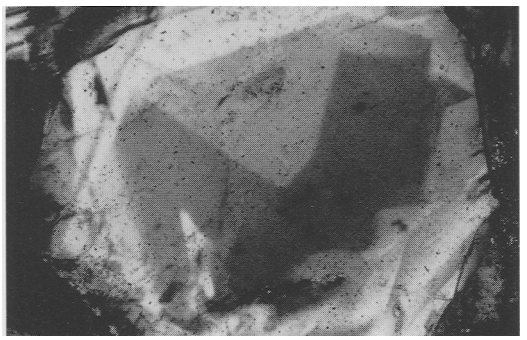

FIG. 1. Photomicrograph of an unaltered eudialyte grain from evolved lujavrite sample (DAR23) under crossed polars. Field of view is 1 mm.

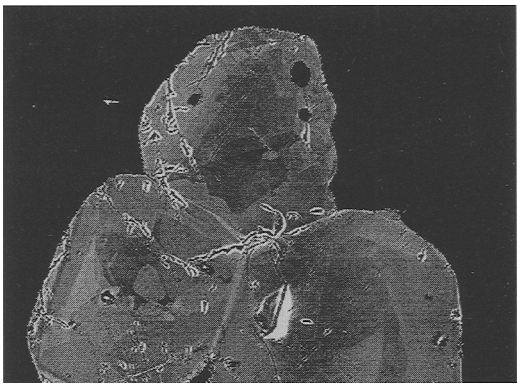

FIG. 2. Back-scattered electron image (BSEI) illustrating subtle but complex zonation in eudialyte from lujavrite sample (DAR24). Note irregular resorbtion near crystal margins. Field of view is 750 μm.

late-stage pegmatite and metasomatized syenite. In the lujavrite eudialyte can reach modal abundances of up to 20% occurring as idiomorphic (~1 mm) crystals. Whereas, in alkali-metasomatized nepheline syenites it occurs in close association with sodalite as large (>2 mm) interstitial, poikiloblastic grains. Representative analyses of eudialyte from North Qôroq, and for comparison, from the adjacent South Qôroq centre are presented in Table 1. The analyses have been recalculated on the basis of 18.5 atoms of oxygen (equivalent to 19 O,OH,Cl,F). The composition of the eudialyte is more Na- than Ca-rich and as the mineral is optically positive can be termed eudialyte *s.s.* as opposed to the Ca-rich end-member of the series, eucolite (Brøgger, 1890; Bollingberg *et al.*, 1983; Deer *et al.*, 1992). This is comparable with eudialyte from the South Qôroq centre.

The larger grains of eudialyte exhibit hour-glass or concentric zoning (Fig. 1) which has been related to variation in minor element content, particularly Ce (*REE*) and Mn (Coulson and Chambers, 1996). This zoning is also visible using back-scattered electron imagery (BSEI, Fig. 2). Smaller eudialyte crystals and the margins of larger grains show more irregular zonation patterns and often resorbtion (see Fig. 2). Coulson and Chambers (1996) proposed that this complex zoning reflects primary magmatic crystallization, overprinted by metasomatic activity.

Chemical variation associated with oscillatory zonation is weakly defined, but there is a slight increase in Ca, *REE* and Mn towards the rim, whereas Na, Si and Fe decrease. Substitutions within North Qôroq eudialyte are small, with only minor systematic changes in Na, Ca, Si and *REE*. The Si shows a negative correlation with Ca and *REE*, and is positively correlated with Na. At crystal margins extensive variation involving Nb and Zr occurs. Niobium reaches 6 wt.% Nb_2O_5 whereas Zr values are much lower than the uniformly high values (11–12% ZrO_2) of the crystal interiors. This erratic variation has been related to metasomatic reactions at the grain margin, and implies that the fluid was capable of mobilizing Nb and Zr (Coulson and Chambers, 1996).

Due to the difficulty in analysing the middle and heavy *REE* using the electron microprobe, mineral separates were obtained and rare earth elements were analysed by inductively coupled plasma spectrometry at Royal Holloway and Bedford New College, University of London, on concentrated lanthanide solutions separated by cation exchange techniques at Birmingham University (after Walsh *et al.*, 1981). The high Nb and *REE* content (Table 2) is reflected in high whole rock values for the sample and eudialyte is seen to be the dominant control of the whole rock *REE* profile (see Fig. 3).

Alteration

The alteration of eudialyte initially takes the form of discolouration along grain boundaries and fractures. This can progress to extensive alteration shown in some examples by resorbtion and modification of crystal margins (Coulson and Chambers, 1996). Ultimately, complete replacement of eudialyte by new pseudomorphing phases occurs. However, it should be stated that entirely altered and unaltered grains can occur in the same thin section (cf. Sørensen, 1962). Figure 4 is a BSEI of secondary phases pseudomorphing eudialyte from the lujavrite within unit SN1B. The diagram also gives the identity (if known) of the pseudomorphing phases. Table 3 shows the chemical composition of some of

TABLE 1. Representative wavelength dispersive electron microprobe analyses of North and South Qôroq eudialyte

Sample	DAR23	DAR24	DAR24	DAR26	DAR26	GGU59661	GGU59661	GGU59663	GGU59663
	Lujavrite	Lujavrite	Lujavrite	Lujavrite	Lujavrite	Pegmatite	Pegmatite	Pegmatite	Pegmatite
Unit	SN1B	SN1B	SN1B	SN1B	SN1B	S. Qôroq	S. Qôroq	S. Qôroq	S. Qôroq
Oxide wt.%									
SiO_2	50.264	47.872	47.979	50.101	51.718	47.590	47.808	46.362	45.708
TiO_2	0.123	n.d.	n.d.	0.140	0.145	n.d.	n.d.	0.088	0.113
ZrO_2	11.998	12.072	11.687	11.937	12.836	11.626	11.702	11.687	11.379
HfO_2	0.258	n.d.	n.d.	0.184	0.265	n.d.	n.d.	0.226	0.267
Nb_2O_5	1.445	1.529	1.545	1.450	0.713	1.944	1.413	2.479	2.994
Al_2O_3	0.295	n.d.	n.d.	0.208	0.155	n.d.	n.d.	0.163	0.142
Y_2O_3	0.477	0.382	0.439	0.434	0.467	0.283	0.324	0.305	0.382
La_2O_3	0.611	0.526	0.579	0.629	0.388	0.348	0.327	0.616	0.803
Ce_2O_3	1.121	0.972	1.081	1.236	0.701	0.853	0.847	1.197	1.393
Pr_2O_3	0.086	0.058	0.049	0.182	0.070	0.120	0.000	0.312	0.130
Nd_2O_3	0.444	0.319	0.352	0.439	0.372	0.271	0.262	0.378	0.463
Sm_2O_3	n.d.	n.d.	n.d.	n.d.	n.d.	n.d.	n.d.	0.246	0.095
FeO	6.531	5.827	6.172	6.385	6.218	6.525	6.620	6.103	6.093
MnO	1.425	1.328	1.421	1.427	1.205	1.488	1.322	2.169	2.466
CaO	10.584	11.004	10.799	11.012	10.595	11.392	11.733	11.661	11.518
Na_2O	10.250	11.871	11.625	9.703	9.407	12.116	11.941	11.328	11.066
K_2O	0.266	0.187	0.164	0.193	0.201	0.149	0.279	0.233	0.254
SrO	0.025	n.d.	n.d.	0.063	0.082	n.d.	n.d.	0.141	0.083
Cl	1.576	1.443	1.441	1.497	1.553	1.230	1.287	1.342	1.243
$-O \equiv Cl$	0.356	0.326	0.325	0.338	0.350	0.278	0.290	0.303	0.280
Total	97.429	95.064	95.008	96.882	96.741	95.657	95.575	96.733	96.312
O	18.5	18.5	18.5	18.5	18.5	18.5	18.5	18.5	18.5
Si	6.567	6.326	6.345	6.546	6.757	6.263	6.288	6.166	6.121
Al	0.049	–	–	0.033	0.032	–	–	0.026	0.023
Ti	0.012	–	–	0.014	0.019	–	–	0.010	0.012
Zr	0.764	0.778	0.754	0.761	0.818	0.746	0.751	0.758	0.743
Hf	0.011	–	–	0.007	0.013	–	–	0.009	0.009
Nb	0.085	0.092	0.093	0.086	0.042	0.116	0.084	0.149	0.181
Fe	0.714	0.644	0.683	0.698	0.679	0.718	0.728	0.679	0.683
Mn	0.158	0.149	0.159	0.158	0.133	0.166	0.147	0.244	0.279
Na	2.597	3.042	2.980	2.458	2.383	3.091	3.045	2.921	2.873
Y	0.033	0.027	0.031	0.030	0.032	0.019	0.022	0.021	0.027
La	0.029	0.025	0.028	0.030	0.019	0.017	0.016	0.030	0.040
Ce	0.054	0.047	0.053	0.059	0.034	0.041	0.041	0.058	0.068
Pr	0.004	0.003	0.002	0.009	0.003	0.006	0.000	0.016	0.007
Nd	0.021	0.015	0.017	0.020	0.017	0.013	0.013	0.018	0.022
Ca	1.482	1.558	1.531	1.542	1.483	1.607	1.653	1.662	1.652
K	0.044	0.031	0.027	0.032	0.034	0.025	0.047	0.040	0.044
Sr	0.002	–	–	0.005	0.008	–	–	0.012	0.010
Cl	0.349	0.323	0.323	0.331	0.344	0.275	0.287	0.303	0.282
Σ	12.975	13.059	13.024	12.819	12.851	13.101	13.121	13.122	13.077

Note: n.d. = not determined, total Fe as FeO

Mineral chemistry was determined using a Cameca Camebax electron microprobe at the University of Edinburgh. Wavelength-dispersion operating conditions were: accelerating voltage 20 kV, beam current 20 nA, a rastered beam covering 12 mm × 12.5 mm. Na was analysed first to minimize decay artefacts.

Synthetic silicate glasses made at the University of Edinburgh were used as standards for *REE*.

La, Ce, Nd and Y were analysed using Lα lines, whereas, for Pr and Sm, Lβ was used. Data reduction was accomplished using PAP correction procedures. Details are presented in Coulson and Chambers (1996).

TABLE 2. Whole rock selected trace element analyses

Sample	DAR24	DAR24	DAR23	DAR25	GGU5966
	Lujavrite	Eudialyte	Lujavrite	Lujavrite	Pegmatite
Unit	SN1B	SN1B	SN1B	SN1B	S. Qroq
(ppm)					
La	316.95	5115.4	124.57	478.95	366.92
Ce	606.96	9737.2	284.07	867.72	741.76
Pr	59.15	916.9	30.65	82.74	70.97
Nd	173.6	2667	94.7	238.1	200.5
Sm	32.3	394.4	15.89	42.77	33.02
Eu	3.18	53	1.51	3.59	4.81
Gd	32.98	393	12.89	40.61	32.58
Dy	41.89	558.1	11.6	47.56	42.87
Ho	10.72	131.7	2.59	12.05	11.02
Er	30.09	364.1	6.29	34.19	32.35
Yb	34.49	413.6	6.76	39.99	34.58
Lu	5.28	62.1	1.04	6.36	5.04
Y	423.8	–	79.2	572.9	392.4
Zr	9121	–	1171	17856	8657
Nb	1070.4	–	267.5	2071.7	1686.7

Note: *REE* were analysed by ICP-AES at Royal Holloway, University of London, see text for details.
Y, Zr and Nb were analysed by XRF techniques at The University of Birmingham. Powdered samples were pressed into pellets and analysed using a Philips PW1400 automated spectrometer. Detailed procedures are available on request.

these secondary minerals, which include, zircon, allanite-(Ce), aegirine, nepheline, natrolite, titanite, several *REE*-bearing silicates of the rinkite, møsandrite and wöhlerite series and an unidentified Nb-silicate phase (Table 3, analysis No. 2). Zirfesite has tentatively been identified (Table 3, analysis Nos 6 and 7), which contrasts with the nearby Ilímaussaq intrusion where it is not seen (Sørensen, 1962).

The zircon is enriched in *REE* and can contain up to 5 wt.% Y_2O_3, whilst the CaTiZr-silicates contain similar abundances of *REE* to eudialyte and may have been formed by fluorination (CaF_2) of eudialyte (with coupled loss of Cl, Zr and SiO_2). Allanite-(Ce), in contrast, contains much higher abundances of *REE* than eudialyte and the other phases present. It occupies only a very minor amount of the original crystal space and can therefore be identified as the major repository for the *REE* as the eudialyte altered, with minor amounts going into the titanite and other silicate minerals. The Zr from the original eudialyte seems to have followed a similar pattern with the bulk of this forming the minor zircon and zirfesite patches. Likewise Nb is incorporated into the unidentified Nb-silicate phase and possibly wöhlerite.

The remaining Na, Ca, Fe and Si from the eudialyte are equally distributed throughout the replacement zone and have been included in nepheline, natrolite, aegirine and the other silicates.

Discussion

Previous work has shown that eudialyte is susceptible to the action of hydrothermal and surface water (e.g. Ussing, 1911), with the spectrum of alteration products having intermediate chemical compositions between eudialyte and zirfesite, the end product of eudialyte alteration under hypergene conditions (Deer *et al.*, 1986). The destruction of eudialyte is accomplished by the loss of Na and Cl and the introduction of water, and if extensive, the loss of SiO_2. This alteration is also accompanied by increasing Zr, Fe and Nb contents (Vlasov *et al.*, 1966).

Several pseudomorphs after eudialyte have been reported in the literature. In Ilímaussaq, secondary minerals after eudialyte include catapleiite, neptunite, aegirine, britholite, monazite, muscovite, biotite, zircon and minor amounts of fluorite, zeolites and sometimes analcite (Boggild, 1953; Sørensen, 1962),

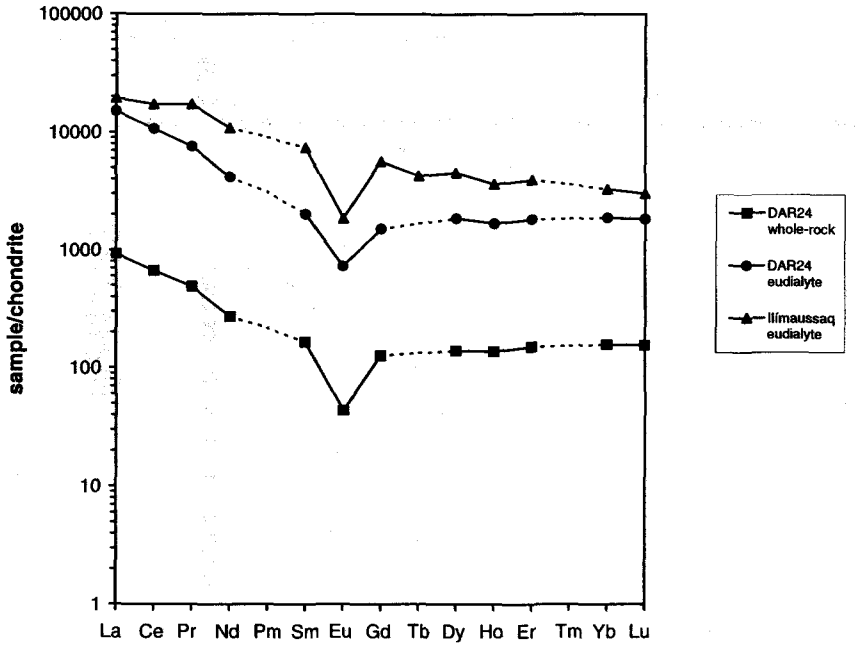

FIG. 3. Chondrite-normalized rare earth element (*REE*) patterns for eudialyte from the lujavrite within unit SN1B, with corresponding whole rock pattern. For comparison the *REE* pattern of eudialyte from Ilímaussaq is included (data from Fryer and Edgar, 1977). Chondritic abundances are those of Wakita *et al.* (1971).

whilst eudialyte relics from Khibina (Dorfman *et al.*, 1963) are present as barsanovite $(Na,Ca,RE)_9(Mn,Fe)_2(Zr,Nb)_2Si_{12}(O,Cl)_{37}$. This appears in rocks in which the nepheline has been cancrinitized and the microcline albitized.

The above description indicates that North Qôroq eudialyte has undergone at least two stages of alteration; the first metasomatic (moderately high-temperature) and the second low-temperature supergene alteration. The high temperature reaction that can be deduced from the observed minerals and from their textures are not well constrained. They include, however, simplified reactions of the form: (1) eudialyte + metasomatic fluid = allanite + nepheline; and (2) eudialyte + metasomatic fluid = titanite + aegirine + møsandrite + wöhlerite.

Depending on the eudialyte compositions and the prevailing f_{O_2} conditions, eudialyte decomposition occurs at temperatures below 800°C, forming nepheline and allanite, or titanite (Ahmed and MacKenzie, 1978). The two reactions above contain all the major constituents in eudialyte pseudomorphs from the North Qôroq centre. Allanite is stable at up to ~750–800°C (Deer *et al.*, 1986; Burt, 1989), and therefore can only have formed below this temperature range, probably as a result of auto-metasomatism within the volatile-rich lujavrite as it cooled. The influx of K and Al from the fluid required for the formation of allanite possibly came from the breakdown of biotite in the rock, or albitization of feldspars (Rae *et al.*, 1996).

This alteration is followed by low-temperature fluid interaction (supergene) with the continued decomposition of the remaining eudialyte into the mineral zirfesite ($Fe_2Zr(SiO_2)_2(OH)$). This is also likely to have been responsible for the discolouration along crystal edges and fractures. A simplified reaction of the form: eudialyte + fluid = zirfesite + fluid is likely to have occurred.

In an attempt to define the alteration of the eudialyte-bearing sample more rigorously, the whole rock composition was compared with an unaltered parent using Gresens' equation for mass balance (Gresens, 1967). This work forms part of a larger study (Coulson, in prep.) defining the metasomatic alteration in the North Qôroq centre. Details of the calculations and methodology used are available from the author and will be presented in a later publication.

Gresens' equation is a simple way of relating change in weight fractions of any given component in a rock to the change in density of the rock, so

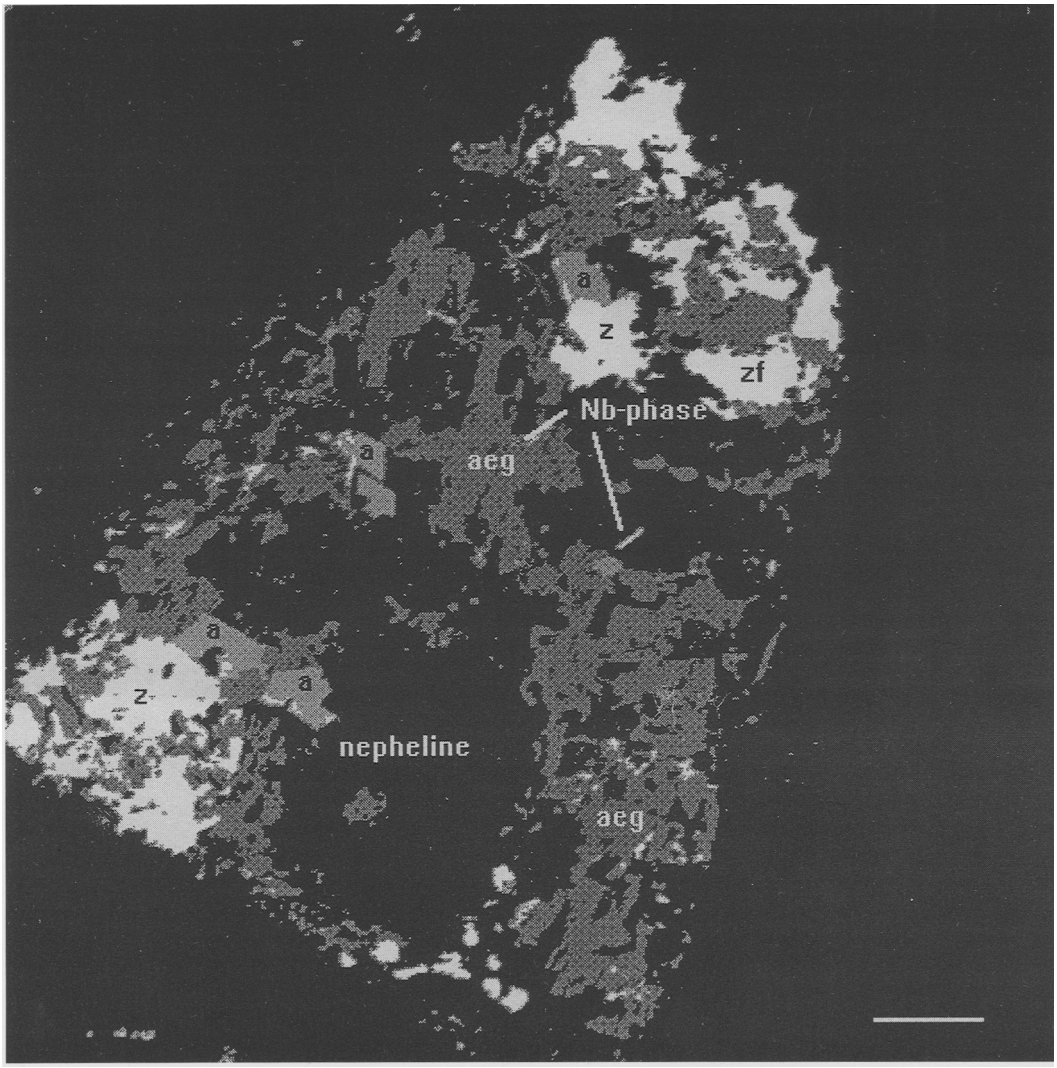

FIG. 4. BSEI of alteration products pseudomorphing eudialyte from lujavrite sample DAR23. z = zircon, zf = zirfesite, a = allanite, aeg = aegirine. Scale bar represents 100 μm.

allowing an estimate of volume change during metasomatism to be made:

$$Xn = 100[Fv(\rho^B/\rho^A)Xn^B - Xn^A]$$

where Xn = the gain or loss of element n in producing metasomatic rock B from parent rock A; Fv = the volume factor, defined as the ratio between the final and initial volumes (i.e. V_B/V_A); $Xn^{A,B}$ = the weight fractions of component n in the parent and metasomatic rock and $\rho^{A,B}$ = the specific gravity of the parent and metasomatic rock.

Figure 5 shows the composition-volume plot for the metasomatized sample DAR23 against a protolith (the average of 2 unaltered lujavrites from the same unit). The Xn-Fv values were calculated for each element at set volume factors of 0.6, 0.8, 1.0, 1.2 and 1.4, corresponding to a range in volume change from 60% of the original volume up to 140% (Table 4). Where the individual lines cut the Xn axis at 0 indicates the element was immobile. If several of the lines crossed the gain-loss zero line at the same value of Fv, Gresens proposed that this 'clustering' can

TABLE 3. Representative wavelength dispersive electron microprobe analyses of North Qôroq eudialyte alteration products

Sample	DAR23 Allanite	DAR23 Nb-silicate	DAR23 Aegirine	DAR23 Nepheline	DAR23 Y-rich zircon	DAR23 Zirfesite	DAR23 Zirfesite	Lovozero Zirfesite† Lujavrite	DAR23 CaTiZr silicate
Oxide wt.%									
SiO_2	33.10	32.17	51.35	44.37	31.69	26.08	22.99	21.27	30.18
ZrO_2	0.11	0.60	0.29	0.04	59.27	44.11	22.75	30.96	2.55
HfO_2	n.d.	n.d.	n.d.	n.d.	n.d.	1.43	0.50	n.d.	n.d.
TiO_2	n.d.	n.d.	n.d.	n.d.	n.d.	n.d.	n.d.	0.96	8.47
Al_2O_3	15.09	8.55	1.65	31.28	n.d.	n.d.	n.d.	1.63	0.05
Y_2O_3	0.00	0.11	0.00	n.d.	5.29	3.33	0.44	n.d.	1.67
La_2O_3	5.64	0.02	0.00	n.d.	0.00	0.10	0.13	n.d.	1.27
Ce_2O_3	10.64	0.14	0.07	n.d.	0.08	0.33	0.85	*2.12	3.49
Pr_2O_3	n.d.	n.d.	n.d.	n.d.	0.03	n.d.	n.d.	n.d.	n.d.
Nd_2O_3	2.58	0.03	0.44	n.d.	0.12	0.12	0.35	n.d.	1.50
Sm_2O_3	0.10	0.13	0.00	n.d.	0.04	n.d.	n.d.	n.d.	n.d.
FeO	15.24	11.02	0.00	1.17	n.d.	n.d.	n.d.	n.d.	n.d.
Fe_2O_3	n.d.	n.d.	32.81	n.d.	0.35	7.03	22.60	14.27	0.62
MnO	1.96	0.28	0.43	0.03	n.d.	n.d.	n.d.	0.24	0.42
Nb_2O_5	0.00	17.65	0.19	n.d.	0.00	n.d.	n.d.	2.40	1.57
CaO	9.61	5.35	0.64	0.03	n.d.	n.d.	n.d.	0.14	32.98
Na_2O	3.28	7.15	13.57	16.47	n.d.	n.d.	n.d.	n.d.	6.67
K_2O	n.d.	n.d.	n.d.	5.14	n.d.	n.d.	n.d.	0.21	0.00
SO_3	n.d.	n.d.	n.d.	0.03	n.d.	n.d.	n.d.	n.d.	n.d.
Cl	n.d.	n.d.	n.d.	0.02	1.29	n.d.	n.d.	n.d.	0.02
F	n.d.	n.d.	n.d.	n.d.	n.d.	n.d.	n.d.	n.d.	6.14
H_2O^+	n.d.	n.d.	n.d.	n.d.	n.d.	n.d.	n.d.	9.66	n.d.
H_2O^-	n.d.	n.d.	n.d.	n.d.	n.d.	n.d.	n.d.	16.17	n.d.
$-O \equiv F,Cl$	–	–	–	0.00	0.29	–	–	–	2.59
Total	97.34	83.19	101.44	98.57	97.86	82.53	70.59	100.11	95.01
O	13	13	6	16	4	4	4	4	24
Si	3.278	3.419	1.979	4.318	1.007	0.976	0.968	0.913	5.799
Zr	0.005	0.030	0.006	–	0.918	0.805	0.467	0.637	0.239
Hf	–	–	–	–	–	0.015	0.006	–	–
Ti	–	–	–	–	–	–	–	0.031	1.225
Al	1.761	1.070	0.075	3.587	–	–	–	0.082	0.011
Y	0.000	0.007	0.000	–	0.089	0.066	0.010	–	0.171
La	0.206	0.000	0.000	–	0.000	–	–	–	0.090
Ce	0.386	0.004	0.002	–	0.001	0.004	0.013	0.033	0.246
Nd	0.091	0.002	0.003	–	0.001	–	–	–	0.103
Sm	0.003	0.004	–	–	–	–	–	–	–
Fe^{2+}	1.262	0.979	0.000	0.095	–	–	–	–	0.100
Fe^{3+}	–	–	0.952	–	0.008	0.198	0.716	0.512	–
Mn	0.164	0.024	0.014	0.002	–	–	–	0.008	0.068
Nb	0.000	0.847	0.008	–	0.000	–	–	0.005	0.136
Ca	1.020	0.609	0.026	0.003	–	–	–	0.006	6.791
Na	0.630	1.473	1.014	3.108	–	–	–	–	2.484
K	–	–	–	0.638	–	–	–	0.001	–
Σ	8.808	8.468	4.000	11.751	2.024	2.064	2.186	2.228	17.463

n.d. = not determined
*Ce_2O_3 represents ΣRE_2O_3
† Zirfesite analysis taken from Vlasov *et al.* (1966)

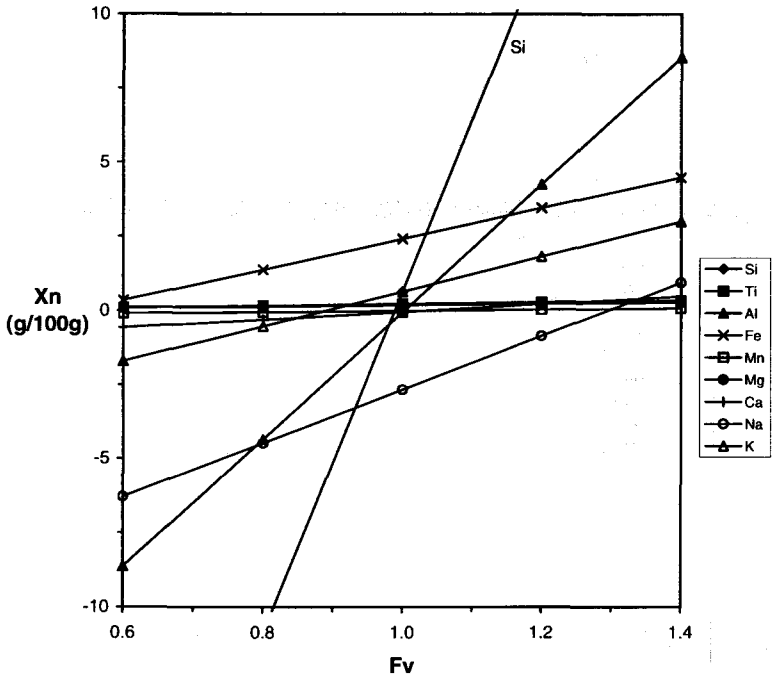

FIG. 5. Composition-volume (Xn-Fv) plot for sample DAR23 against protolith from unit SN1B. Fv values of 0.6, 0.8, 1.0, 1.2 and 1.4 are substituted into Gresens' (1967) equation and corresponding values of Xn are calculated for each component.

indicate that those elements constitute a group of immobile elements and the unique Fv value deduced can be applied to the other mobile elements to calculate the gains and losses. The basis for this is simply that it is unlikely that a group of elements would behave identically if they were all mobile. However, Appleyard and Woolley (1979) and Appleyard (1980) suggest that in some instances elements will behave in an identical fashion and other evidence should be sought in order to confirm this grouping.

It is interesting to note that several of the element lines cut $Xn = 0$ at close to Fv 1.0, which corresponds to zero volume change (constant volume). These elements include Si, Ca and Al, of which Al is commonly taken to be immobile during metasoma-

TABLE 4. Calculated Xn-Fv values for sample DAR23 from Gresens' (1967) equation

Calculated Xn-Fv Sample DAR23 Fv	Si	Ti	Al	Fe_T	Mn	Mg	Ca	Na	K
							density protolith = 2.551 density sample = 2.556		
0.6	−22.50	0.11	−8.65	0.35	−0.10	0.09	−0.57	−6.29	−1.71
0.8	−10.93	0.17	−4.35	1.38	−0.05	0.13	−0.31	−4.48	−0.53
1.0	0.65	0.22	−0.06	2.41	−0.01	0.18	−0.05	−2.67	0.64
1.2	12.22	0.28	4.24	3.44	0.03	0.23	0.22	−0.86	1.82
1.4	23.79	0.34	8.54	4.47	0.07	0.27	0.48	0.94	2.99

Major element data taken from Coulson (unpublished data)

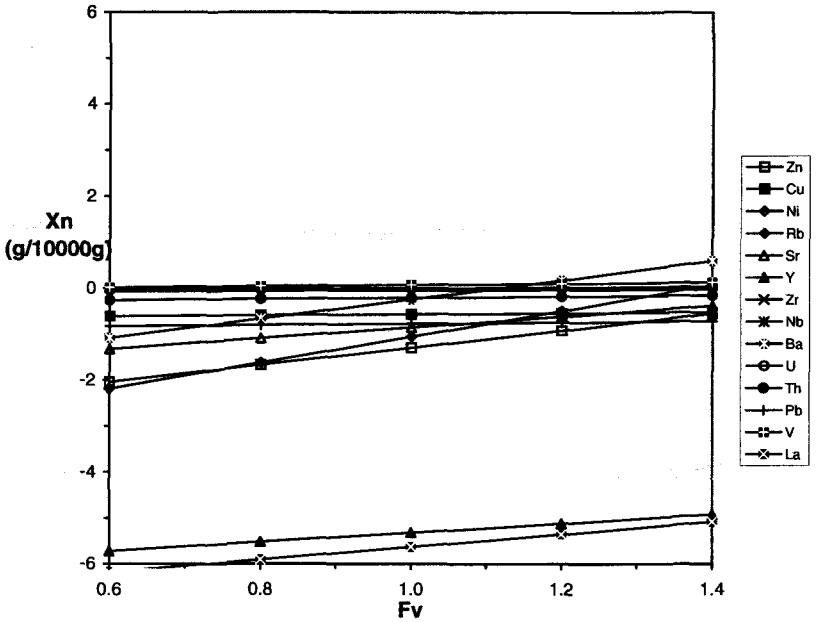

FIG. 6. Corresponding composition-volume (X*n*-Fv) plot for trace elements from sample DAR23 against protolith from unit SN1B.

tism of felsic rocks (Rubie, 1982; Rubie and Gunter, 1983). This Fv agrees with petrographic observations of constant volume (i.e. lack of veining, pseudomorphs), and can be taken as a further line of evidence for the accuracy of using this equation as a model for defining metasomatic alteration. The plot shows that at near constant volume there is an increase in Fe (+2.41 g/100g) and a slight increase in Si and K (+0.65 and +0.61 g/100g), whilst Na is the only significant element to decrease (−2.67 g/100g). Figure 6 is the corresponding plot for trace elements. What is noticeable is that all trace elements are lost from the systems (at reasonably realistic volume factors) and that most noticeably La, Y, Nb and Zr are significantly depleted (−5.6 to −166 g/10000g at Fv 1.0). The only element on the plot seen to gain is Ba and this is only at a volume factor of 1.2, representative of a volume increase of 20%, which clearly contradicts petrographic evidence. Therefore it can be stated that metasomatism took place at near constant volume with only small gains and losses in major elements (namely increase in Fe, loss of Na) and extreme trace element (particularly *REE*, Nb and Zr) loss from the sample. This implies that the alteration of eudialyte (the major repository for Na, *REE*, Y, Zr and Nb) took place with most of the constituent elements being lost to the fluid and only Fe being introduced, which was incorporated into the new mineral zirfesite. The remaining quantities of trace elements within the eudialyte went on to make up the allanite and other psuedomorphing phases. One concluding point to note is that metasomatized quartzite xenoliths above the lujavrite are highly enriched in *REE* (>20,000 ppm whole rock). Presumably this acted as a sink for the products of eudialyte alteration (Rae *et al.*, 1996).

The above whole rock data seem to support the other data (i.e. mineral analyses) that Na is lost from the North Qôroq eudialyte during alteration. This may explain why other more common alteration products of eudialyte, the complex Na-Zr-silicates (namely catapleiite, lovozerite and steenstrupine: Sørensen, 1962; Vlasov *et al.*, 1966; Bollingberg *et al.*, 1983) are not present in North Qôroq. North Qôroq fluids are not as peralkaline (persodic) as those at Ilímaussaq and hence these Na-Zr-rich products will not be observed/preserved.

Conclusions

Pristine euhedral eudialyte from North Qôroq is a product of residual magmatic crystallization. It is seen to alter readily and, commonly, pseudomorphs after eudialyte are formed by secondary minerals.

This new mineral assemblage has come about as the result of two stages of post-magmatic fluid

interaction. The first, soon after crystallization, is metasomatic alteration, related to the cooling of the volatile rich magma, or fluids from later intrusions, which produced the high temperature replacement assemblage (e.g. allanite, zircon). The second less aggressive fluid is supergene in origin and lower temperature, which aided the continued decomposition of eudialyte to the mineral zirfesite. This alteration took place at near constant volume with the loss of Na and trace elements (particularly *REE*, Y, Zr and Nb) and only minor introduction of Fe into the system.

Fresh unaltered grains occur with completely altered eudialyte in the same thin section, indicating that fluids responsible for this alteration were not pervasive. The elements Zr, Nb, Y and *REE* were shown to be mobile in the fluid phase.

Acknowledgements

Original fieldwork on the North Qôroq centre was supported by the Geological Survey of Denmark and Greenland, and results on Survey material appear by permission of the Director. Research for the current work was carried out during tenure of a postgraduate studentship from NERC. I am grateful to A.D. Chambers for his supervision and introduction to the subject. J.R. Ashworth is thanked for his helpful and constructive comments on an earlier version of the manuscript. This work has benefited from the careful and critical reviews of F. Wall and A. Finch. The assistance of G.L. Hendry (Birmingham), P. Hill and S. Kearns (University of Edinburgh) and S. James and N. Walsh (Royal Holloway, University of London) with various aspects of analytical work is gratefully acknowledged.

References

Ahmed, M. and MacKenzie, W.S. (1978) Preliminary report on the synthesis and stability of eudialyte. *Progress in Experimental Petrology, Fourth Report* 1975–8, 47–9. NERC.

Appleyard, E.C. and Woolley, A.R. (1979) Fenitization: an example of the problems of characterizing mass transfer and volume changes. *Chem. Geol.*, **26**, 1–15.

Appleyard, E.C. (1980) Mass balance computations in metasomatism: Metagabbro/nepheline syenite pegmatite interaction in northern Norway. *Contrib. Mineral. Petrol.*, **73**, 131–44.

Bøggild, O.B. (1953) The mineralogy of Greenland. *Medd. øm Grønland,* **149;3**, 251 pp.

Bollingberg, H.J., Ure, A.M., Sørensen, I. and Leonardsen, E.S. (1983) Geochemistry of some eudialyte-eucolite specimens and a co-existing catapleiite from Langesund, Norway. *Tschermaks Min. Petr. Mitt.*, **32**, 153–69.

Brøgger, W.C. (1890) Die Mineralien der südnorwegischen Augit- und Nephelin Syenite. *Z. Kristallogr.*, **16**, II.

Burt D.M. (1989) Compositional and phase relations among rare earth element minerals. In *Geochemistry and Mineralogy of Rare Earth Elements* (B.R. Lipin and G.A. McKay, eds). Mineralogical Society of America, *Reviews in Mineralogy*, **21**, 259–307.

Coulson, I.M. and Chambers, A.D. (1996) Patterns of zonation in patterns in rare-earth bearing minerals in nepheline syenites of the North Qôroq centre, South Greenland *Can. Mineral.*, **34(6)**, (in press).

Deer, W.A, Howie, R.A. and Zussman, J. (1986) *Rock-Forming Minerals - Volume 1B Disilicates and Ring Silicates (2nd ed.).* Longman Scientific & Technical, Harlow, England.

Deer, W.A, Howie, R.A. and Zussman, J. (1992) *An Introduction to the Rrock-Forming Minerals (2nd ed.).* Longman Scientific & Technical, Harlow, England, 696 pp.

Dorfman, M.D., Ilokhim, V.V. and Burova, T.A. (1963) [Barsanovite — a new mineral.] *C. R. Acad. Sci., USSR*, **153**, 1164–67 (in Russian).

Emeleus, C.H. and Harry, W.T. (1970) The Igaliko Nepheline syenite complex: general description. *Medd. øm Grønland,* **186;3**, 115 pp.

Fryer, B.J. and Edgar, A.D. (1977) Significance of rare-earth distributions in coexisting minerals of peralkaline undersaturated rocks. *Contrib. Mineral. Petrol.*, **61**, 35–48.

Gresens, R.L. (1967) Composition-volume relationships of metasomatism. *Chem. Geol.*, **2**, 47–55.

Jones, A.P. and Larsen, L.M. (1985) Geochemistry and *REE* minerals of nepheline syenites from the Motzfeldt centre, South Greenland. *Amer. Mineral.*, **70**, 1087–100.

Jones, A.P., Wall, F. and Williams, C.T. (eds.) (1996) *Rare Earth Minerals: Chemistry, Origin and Ore Deposits.* The Mineralogical Society Series **7**, Chapman and Hall, London, 372 pp.

Khomyakov, A.P. (1990) *Mineralogy of Hyperagpaitic Alkaline Rocks*, Science Press, Moscow, 196 pp (in Russian). Translated into English as Khomyakov, A.P. (1995) *Mineralogy of Hyperagpaitic Alkaline Rocks*, Clarendon Press, Oxford, 233 pp.

Mellini, M. and Merlino, S. (1979) Refinement of the crystal structure of wöhlerite. *Tschermaks Min. Petr. Mitt.*, **26**, 109–23.

Petersen, O.V., Rønsbo, J.G. and Leonardsen, E.S. (1989) Nacareniobsite-(Ce), a new mineral species from the Ilímaussaq alkaline complex, South Greenland, and its relation to møsandrite and the rinkite series. *Neues Jahrb. Mineral. Mh.*, **2**, 84–96.

Rae, D.A., Coulson, I.M. and Chambers, A.D. (1996) Metasomatism in the North Qôroq centre, South Greenland: apatite chemistry and rare-earth element

transport. *Mineral. Mag.*, **60**, 207–20.

Rubie, D.C. (1982) Mass transfer and volume change during alkali metasomatism at Kisingiri, Western Kenya. *Lithos*, **15**, 99–109.

Rubie, D.C. and Gunter, W.D. (1983) The role of speciation in alkaline igneous fluids during fenite metasomatism. *Contrib. Mineral. Petrol.*, **82**, 165–75.

Sørensen, H. (1962) On the occurrence of steenstrupine in the Ilímaussaq massif, southwest Greenland. *Medd. øm Grønland,* **32;1**, 251 pp.

Upton, B.G.J. and Emeleus, C.H. (1987) Mid Proterozoic alkaline magmatism in southern Greenland. In *Alkaline Igneous Rocks* (J.G. Fitton and B.G.J. Upton, eds.). *Spec. Publ. Geol. Soc., London*, **30**, 449–71.

Ussing, N.V. (1911) Geology of the country around Julianehaab. *Medd. øm Grønland,* **38**, 376 pp.

Vlasov, K.A., Kuz'menko, M.Z. and Es'kova, E.M. (1966) *The Lovozero Alkali Massif.* Oliver and Boyd, Edinburgh and London, 627 pp.

Watika, H., Rey, P. and Schmitt, R.A. (1971) Abundances of the 14 rare-earth elements and 12 other trace elements in Apollo 12 samples: five igneous and one breccia rocks and four soils. *Proc. 2nd Lunar Sci. Conf.*, pp. 1319–29.

Walsh, J.N., Buckley, F. and Barker, J. (1981) The simultaneous determination of the rare-earth elements in rocks using inductively coupled plasma source spectrometry. *Chem. Geol.*, **33**, 141–53.

[*Manuscript received 26 February 1996: revised 2 July 1996*]